JOURNAL OF MATERIALS SCIENCE **34** (1999) 4511–4518

Effect of small amount of alumina doping on superplastic behavior of tetragonal zirconia

E. SATO, H. MORIOKA, K. KURIBAYASHI, D. SUNDARARAMAN*
The Institute of Space and Astronautical Science, 3-1-1 Yoshinodai, Sagamihara, 229-8510, Japan
E-mail: sato@materials.isas.ac.jp

The effect of Al_2O_3 doping of around 0.1 wt% on superplastic behavior was studied in 3 mol% yttria-stabilized tetragonal zirconia polycrystal (TZP) which was free from SiO_2 contamination and had a grain size of 0.4 μm. Compression creep tests revealed that high-purity TZP with less than 0.07 wt% Al_2O_3 had two deformation regions: the low stress region had a stress exponent of three and an apparent activation energy of 640 kJ/mol, and the high stress region had two and 460 kJ/mol. On the other hand, TZP containing more than 0.12 wt% Al_2O_3 had only one region which had a stress exponent of two and an activation energy of 480 kJ/mol. The region of diffusion control with a stress exponent of one was not observed in any samples. High resolution transmission electron microscopy revealed that no amorphous grain boundary phase was produced even with 0.18 wt% Al_2O_3 doping. Energy dispersive X-ray spectroscopy near grain boundaries revealed that yttrium was segregating at the grain boundaries with denuded zones of 30 nm width, which were created during slow cooling from the sintering temperature.

1. Introduction

Since the discovery of superplasticity in yttria-stabilized tetragonal zirconia (TZP) [1], there have been numerous studies [2] on the superplastic behavior of monolithic TZP [3–10], Y-TZP with a glassy phase [11–14] and alumina/TZP composites [15–17]. The parameters such as the stress exponent $n \equiv \partial \ln \dot{\varepsilon} / \partial \ln \sigma$, the apparent activation energy $Q \equiv R \partial \ln \dot{\varepsilon} / \partial (1/T)$ and the grain size exponent $p \equiv \partial \ln \dot{\varepsilon} / \partial \ln d$ characterize the steady-state deformation of superplasticity, where $\dot{\varepsilon}$ is the strain rate, σ is the stress, T is the temperature and d is the grain size. The early studies on monolithic Y-TZP showed disparate values of the stress exponent of two [1, 3] and three [6, 7]. Similar discrepancy was also reported for the activation energy [3, 7]. Later it was suggested that the change in the stress exponent is related to the impurity content of the material, i.e., high-purity TZP shows a stress exponent of three while low-purity material shows two [8, 9]. In addition, another region at high stresses with a stress exponent of one was reported in both high- and low-purity materials [8, 9]. However, another study claimed the absence of the highset stress region with a stress exponent of one [2, 10]. In contrast to such confusions in monolithic TZP, in TZP with another phase, such as the glassy phase [11–14] or alumina [15–17], only one region with a stress exponent of two was reported.

The above flow behavior should be influenced by the atomic structure and chemical composition of the grain boundaries. In high-purity TZP, clean grain boundaries without an amorphous phase were observed using high resolution electron microscopy (HREM) [7, 18, 19], while the existence of amorphous phases at grain boundaries was reported in low-purity TZP using conventional transmission electron microscopy (TEM) [18] and in TZP with a glassy phase using HREM [14]. However, recently, even in TZP with a glassy phase, clean grain boundaries absent of a grain boundary amorphous phase (film) were observed by HREM [20].

The mechanism of superplasticity involves grain boundary sliding with grain switching [21], and the sliding rate is controlled by accommodation processes, i.e., diffusion creep in materials with clean grain boundaries [21, 22] and solution-precipitation creep in materials with a grain boundary glassy phase [23]. Both diffusion creep and solution-precipitation creep can be controlled either by diffusion [21, 23] or by interface reaction [22, 23]. Recently, Wakai [24] proposed a precise formulation of solution-precipitation creep based on the classical crystal growth theory [25] in order to explain the experimental results of low-purity TZP: the existence of a grain boundary glassy phase and the transition from a stress exponent of two at low stresses to one at high stresses. Recent reports of the absence of a glassy phase [20] and the absence of the highest stress region [2, 10] requires reconsideration of the theoretical scheme of solution-precipitation creep [24].

* On leave from Indira Gandhi Centre for Atomic Research, Kalpakkam, TN, India.

In the present study, superplastic flow behavior was examined over a wide range of strain rate and temperature in TZP doped with several amounts of alumina in order to clarify the role of impurities on the rate-controlling processes of the superplastic flow. The grain boundary microstructure was also characterized using HREM and energy dispersive X-ray spectroscopy (EDS). Alumina was selected as a controlled dopant because many of the present commercial TZPs contain less than 0.01 wt % silica and soda but contain about 0.2 wt % alumina as a sintering aid [5].

2. Experimental

Raw materials were undoped 3Y-TZP powder (TZ-3Y, Tosoh Co., Ltd.) and 3Y-TZP powder doped with 0.18 wt % alumina (TZ-3Y-E, Tosoh Co., Ltd.). Four kinds of 3Y-TZP powders containing various amount of alumina were then prepared through ball mixing of undoped TZP powder and pure alumina powder (TM-DAR, Taimei Chem. Co., Ltd.) using a pot and balls made of alumina. The main chemical compositions of the prepared powders are listed in Table I. Other impurities were typically 0.006 wt %SiO_2, 0.003 wt %Fe_2O_3 and 0.002 wt %Na_2O. Although silica is an impurity easy to be introduced during treating the powders, it remained below 0.02 wt %SiO_2 after ball mixing.

Dense cylindrical samples of 6 mm diameter and 8 mm length were prepared from these powders through cold isostatic pressing at 400 MPa, air sintering at 1673 K for 2 h with heating and cooling rates of 10 K/min, and polishing of the bases. Scanning electron microscopy (SEM) on the thermal edged surface revealed that the above sintering condition resulted in a grain size of 0.4 μm. High temperature compression tests were performed with an Instron type machine equipped with an SiC jig in air at temperatures from 1473 to 1773 K with strain rates from 1.25×10^{-6} to 1.0×10^{-3} s^{-1}.

TEM samples for the as-sintered materials were prepared from a mechanically cut disk of 3 mm diameter without support rings through dimpling and Ar ion milling with an accelerating voltage of 4 kV and a glancing angle of 10° followed by C coating. These samples were free from contamination of sputtered material from the support rings during ion milling. High resolution observations were performed using JEM-3010 (300 kV, LaB_6 filament) and JEM-ARM1250 (1250 kV, LaB_6 filament). EDS analysis near the grain boundaries was performed with an EDAX DX-4 system attached to a JEM-3010 under a nano beam mode with a spot size 2 nm.

3. Results

3.1. Compression tests

Fig. 1a shows the stress and strain rate relations in undoped TZP at 1473, 1573, 1673 and 1773 K. The stress exponent is three at low stresses and two at high stresses. It is clear that the transition is from a stress exponent of three to two but not from three to one. The apparent activation energy is 638 kJ/mol at low stresses and 461 kJ/mol at high stresses.

Fig. 1b shows the stress and strain rate relations in $0.18Al_2O_3$-TZP. The stress exponent of two is observed all over the measured region and no region of one is observed. The apparent activation energy is 481 kJ/mol, which is close to that at high stresses in undoped TZP.

In Fig. 2, the data at 1673 K in TZP of various doping levels are summarized. They can be classified into two groups according to the doping levels: the samples of doping level below 0.07% show two regions, a stress exponent of two at high stresses and three at low stresses, while the samples of doping level above 0.12 wt % show only one region with a stress exponent of two. The high-purity group shows a lower strain rate than the low-purity group, and the difference becomes larger at lower stresses.

3.2. Electron microscopy

Fig. 3a and b are high resolution electron micrographs of one grain boundary in as-sintered $0.18Al_2O_3$-TZP enlarged from one negative; Fig. 3b is placed left of Fig. 3a. The grain boundary in Fig. 3 is a high angle, random boundary. The lattice fringes of both grains meet at the grain boundary directly as seen in Fig. 3a, showing the absence of a grain boundary glassy phase. No intergranular precipitation nor dislocation is observed. Along the grain boundary, the atomic structure is distorted in the width of 0.4 nm. On the other hand in Fig. 3b, along the grain boundary, a darkened band of 5 nm width is observed. Because we can see lattice fringes inside of this band, it is not the grain boundary glassy phase but a grooved region created by damage from ion milling. In the bright field mode and Fresnel fringe mode, this band shows a thickness contrast, which looks like a grain boundary glassy phase similar to Figs 2 and 3 in Ref. [18].

Since the sample was cooled down with a rather small cooling rate of 10 K/min, redistribution of the segregated yttrium happened, as discussed in detail in Section 4.4. We cannot rule out the possibility that independent phases such as dispersoids or a grain boundary glassy phase, which might be more stable than the independent yttrium ions, were also affected by the cooling

TABLE I Chemical compositions of the prepared powders

Powders	Non-doped	$0.03Al_2O_3$	$0.07Al_2O_3$	$0.12Al_2O_3$	$0.18Al_2O_3$	$0.95Al_2O_3$
Y_2O_3 (wt %)	5.11	5.11	5.11	5.11	5.02	5.11
Al_2O_3 (wt %)	0.005	0.032	0.073	0.12	0.18	0.95

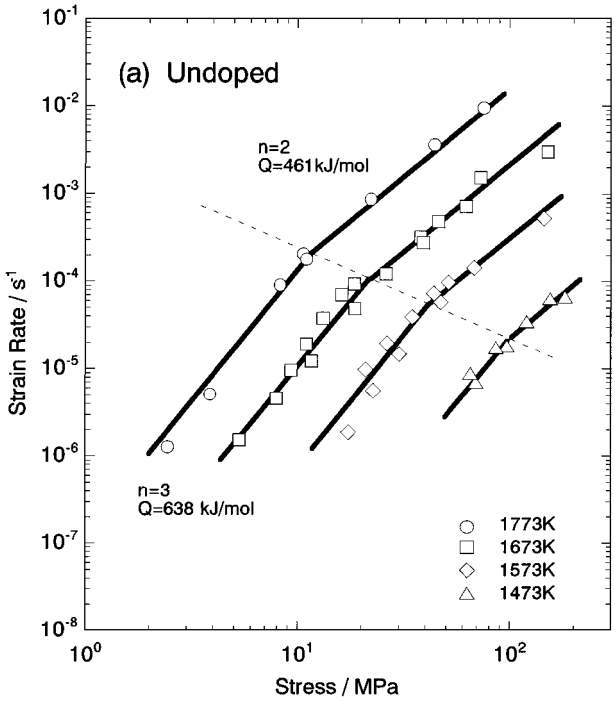

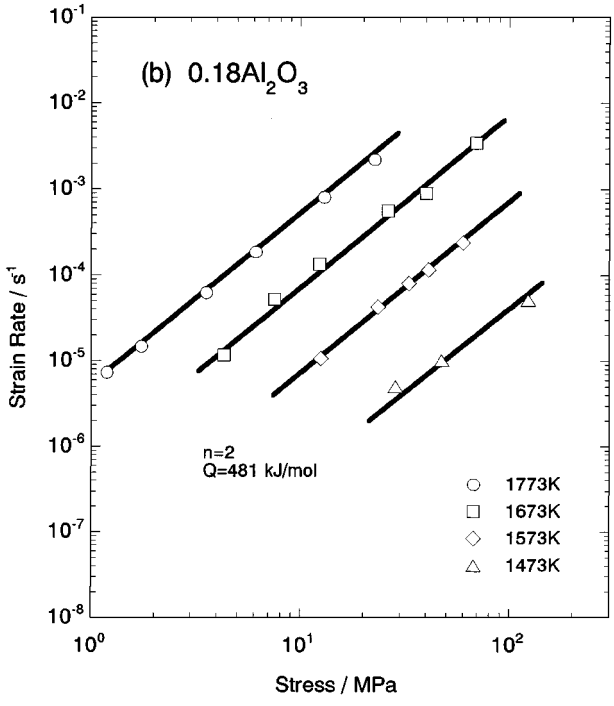

Figure 1 Stress and strain rate relations in (a) undoped and (b) $0.18Al_2O_3$-TZP at 1473, 1573, 1673 and 1773 K. In undoped TZP, two regions, a stress exponent of two at high stresses and three at low stresses, are distinguished; in $0.18Al_2O_3$-TZP only one region of a stress exponent of two is seen.

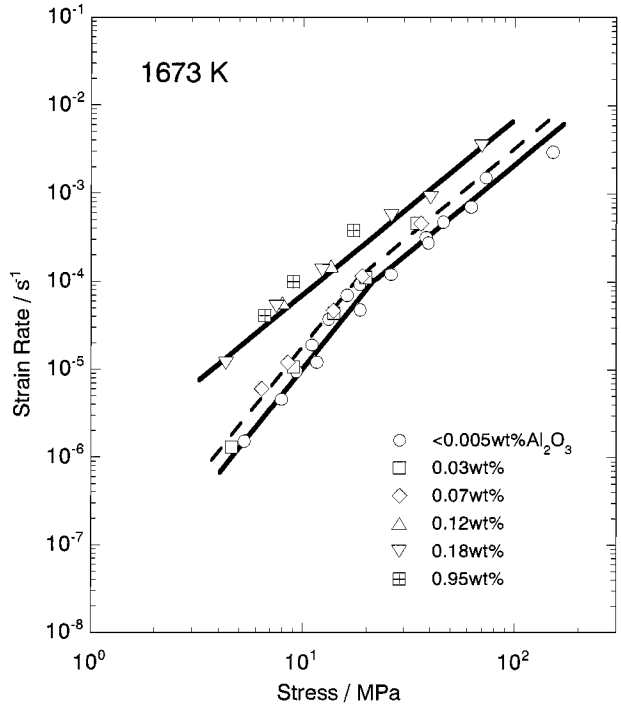

Figure 2 Stress and strain rate relations in TZP with various levels of Al_2O_3 doping at 1673 K. The samples of doping level below 0.07% show two regions, a stress exponent of two at high stresses and three at low stresses, while the samples of doping level above 0.12 wt % show only one region with a stress exponent of two.

procedure. However, the point of the observation is that the different features are observed in the neighboring places of one grain boundary.

Fig. 4 is a high resolution electron micrograph of a grain boundary triple point in $0.18Al_2O_3$-TZP. The lattice fringes of the three grains meet directly with some amount of overlapping caused by the insufficient edge-on condition of the boundaries. Almost all of the observed triple points possessed no glass pocket like this micrograph. Very few triple points had a glassy pocket of the size of 5 nm. EDS analysis revealed that this glassy phase consisted of 13 wt %SiO_2, 9 wt %Y_2O_3, 5 wt %Al_2O_3 and the balance of ZrO_2, indicating that impurity silica was localized to form silicate glass. Because the samples studied in this study contained impurity silica of about 0.006 wt %, the effect of the glassy pocket on deformation behavior was neglected.

For many grain boundaries (more than ten) in $0.18Al_2O_3$-TZP, EDS analysis with a spot size of 2 nm was performed. Only the yttrium distribution was analyzed using the Y L peak and the Zr L peak because the Al K peak was overlapped by lower energy side of the Zr L peak. Fig. 5a shows that Y is segregating in the grain boundaries and that denuded zones with a width of 30 nm are formed around the grain boundaries . This yttrium segregation and denuded zone are also observed in $0.18Al_2O_3$-TZP sintered at 1773 K for 10 h, as shown in Fig. 5b.

4. Discussion

4.1. Comparison with the recent data

The present data on flow behavior are compared with the recently reported data of two categories in TZP with a grain size about 0.4 μm; while Lakki *et al.* [9] and Wakai *et al.* [5] reported a transition from $n = 3$ or 2 to 1 in high- or low-purity materials, respectively, Owen and Chokshi [10] reported a transition only in high-purity materials from $n = 3$ to 2. The data are normalized to those at 1673 K and of 0.4 μm grain size using the apparent activation energy $Q = 480$ kJ/mol and the grain size exponent $p = 2$ (for the $n = 2$ region) and $Q = 640$ kJ/mol and $p = 1$ (for the $n = 3$ region).

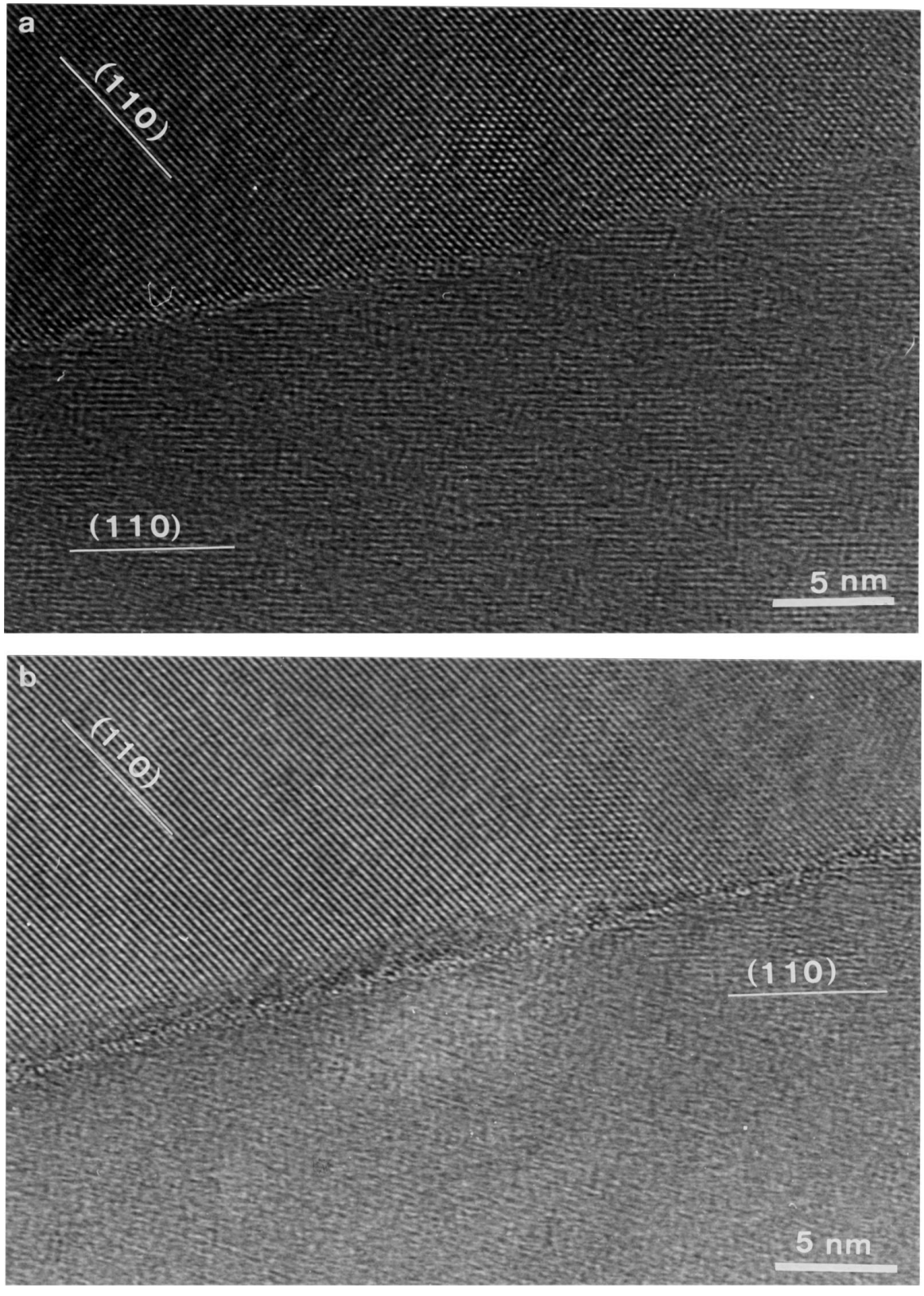

Figure 3 High resolution electron micrographs of one grain boundary in $0.18Al_2O_3$-TZP enlarged from one negative. (a) The lattice fringes of both grains meet at the grain boundary directly, showing the absence of a grain boundary glassy phase. (b) Along the grain boundary, a darkened band of 5 nm width is observed. We can see lattice fringes inside of this band; therefore it is not the grain boundary glassy phase but is a grooved region created by damage from ion milling.

All the data show good agreement except those in the high stress region ($n = 2$) in high-purity TZP, indicated by the closed symbols in Fig. 6a. In that region, the present data locate just between those of Lakki *et al.* [9] and Owen and Chokshi [10], and the data for each study seem to lie on a respective line of $n = 2$ but not on a line of $n = 1$. The region of $n = 1$ at high stresses, which is based on a few data points in Ref. [8, 9], is absent at least up to 200 MPa both in high- and low-purity TZP with a grain size of about 0.4 μm.

This conclusion, however, does not deny the existence of the region of $n = 1$ at higher stresses, where

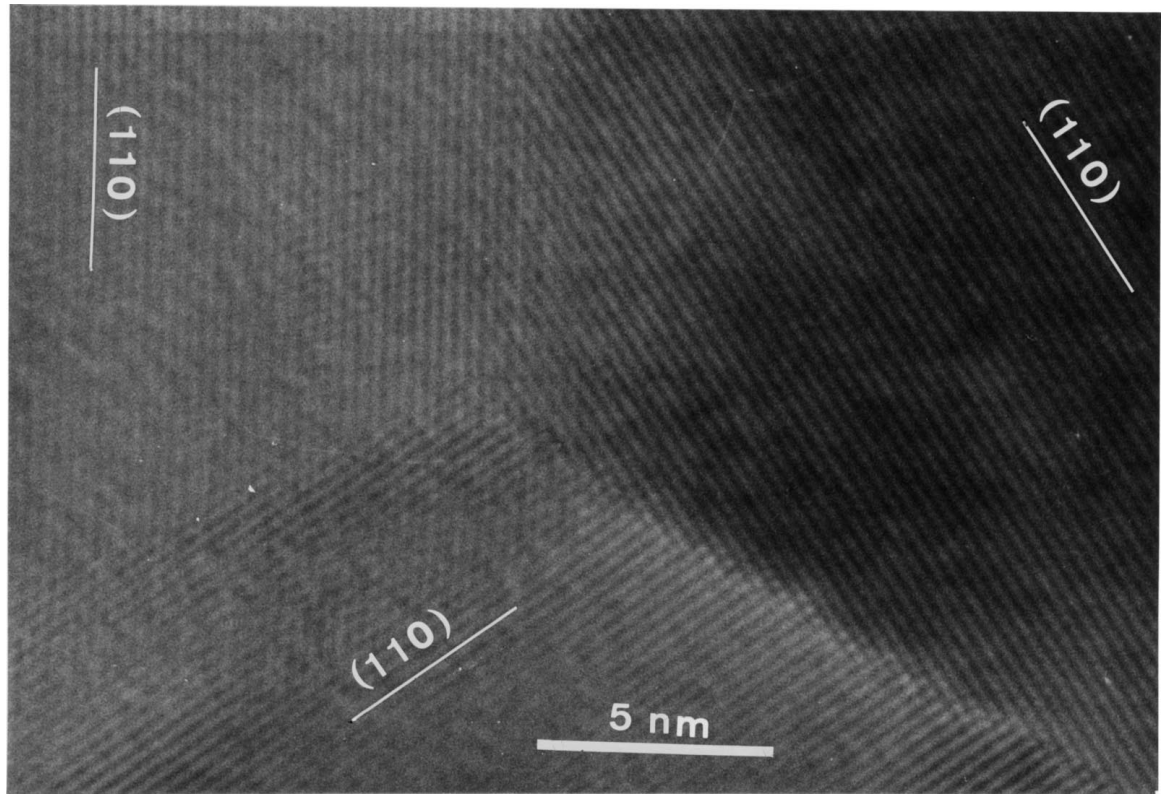

Figure 4 High resolution electron micrograph of the grain boundary triple point in $0.18Al_2O_3$-TZP, indicating that the lattice fringes of three grains meet directly without forming a glass pocket.

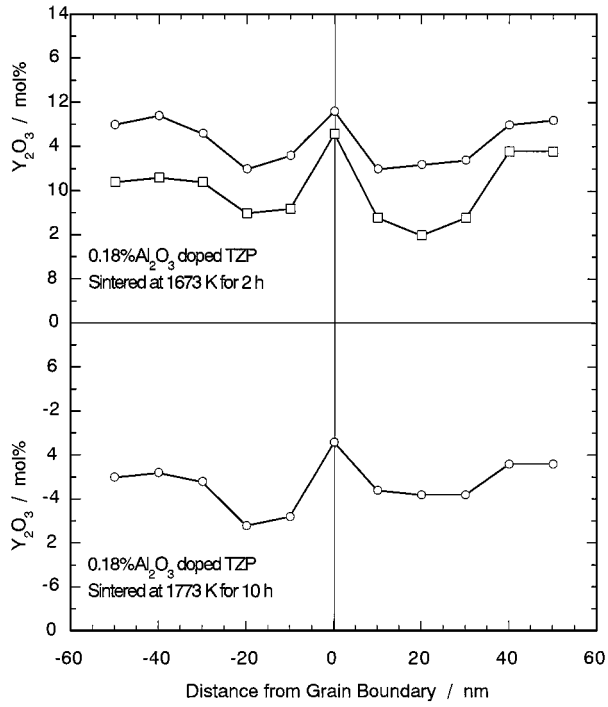

Figure 5 Profiles of Y distribution across the grain boundaries in $0.18Al_2O_3$-TZP sintered at 1673 K for 2 h (a) and 1773 K for 10 h (b). Both specimens show that Y is segregated in the grain boundaries and around the grain boundaries, denuded zones with a width of 30 nm are formed.

deformation might be controlled by diffusion. The constitutive equation for grain boundary sliding with grain switching controlled by diffusion is given as [21]

$$\dot{\varepsilon} = 329\frac{\Omega}{kT}D_{gb}\frac{\sigma\delta}{d^3}, \quad (1)$$

where $\Omega = 0.7b^3$ is the molar volume, $b = 2.57 \times 10^{-10}$ m is Burger's vector [26], $\delta = 2b$ is the grain boundary width and kT has the usual meaning. The grain boundary diffusion coefficient D_{gb} is assumed to equal to that for cubic zirconia, $2.3 \times 10^{-3}\exp[-293\,\text{kJ mol}^{-1}/RT]\ \text{m}^2\ \text{s}^{-1}$ measured by Oishi *et al.* [27]. This equation predicts that the diffusional control appears under a stress of more than 3×10^3 MPa in TZP of 0.4 μm at 1673 K.

On the other hand, Kusunoki and Ikuhara [28] reported a smaller value of $D_{gb} = 1.1 \times 10^3\ \text{m}^2\ \text{s}^{-1}$ (at 1673 K) through *in situ* observation at high temperatures in TEM. This diffusion coefficient predicts that almost all of the measured data fall under the region of diffusional control. A creep study at still higher stresses would provide information on this large discrepancy in the diffusion constant.

Just recently, an interpretation that a temperature-depending threshold stress causes the increase in a stress exponent from two to three with decreasing the stress in low-purity TZP [29]. We cannot, unfortunately, affirm nor deny the temperature-depending threshold mechanism considering the experimental errors of the present data and their data. Before the further discussion on the threshold mechanism, it is required to propose the origin of the threshold stress which depends on the temperature and grain size.

4.2. Change in strain rate with doping

The effect of doping level on the strain rate is plotted in Fig. 7a using a double logarithmic plot. The plotted data are at 30 MPa for the $n = 2$ region and 5 MPa for

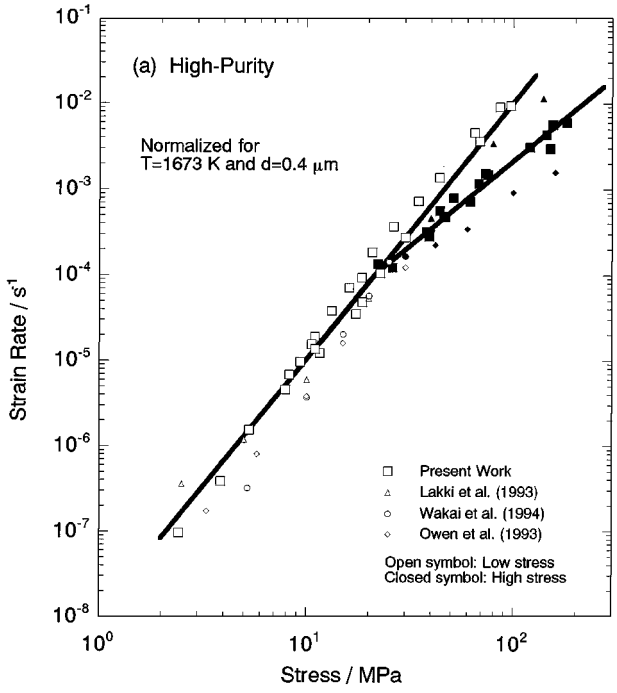

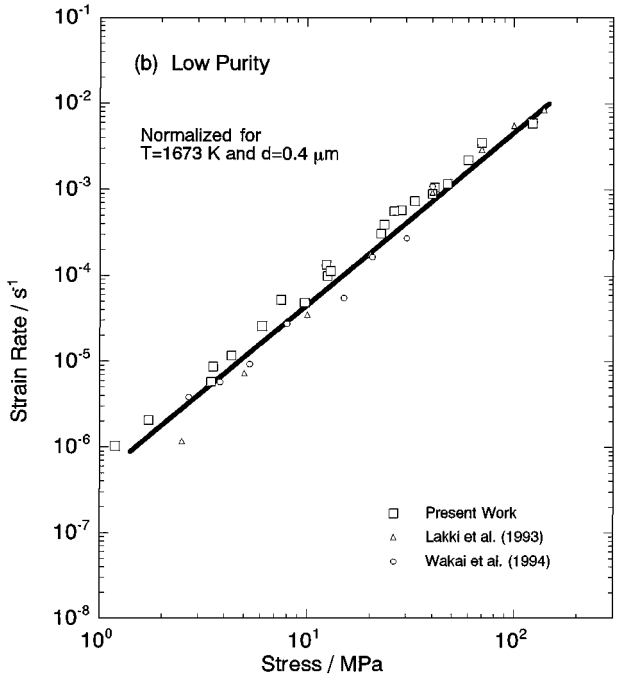

Figure 6 Comparison between the present study and the recently reported study of two categories; while Lakki *et al.* [9] and Wakai *et al.* [5] reported a transition from $n = 3$ or 2 to 1 in high- or low-purity materials, respectively, Owen and Chokshi [10] reported a transition only in high-purity materials from $n = 3$ to 2. The data are normalized into those at 1673 K and with grain size of 0.4 μm using $Q = 480$ kJ/mol and $p = 2$ (for the $n = 2$ region) and $Q = 640$ kJ/mol and $p = 1$ (for the $n = 3$ region).

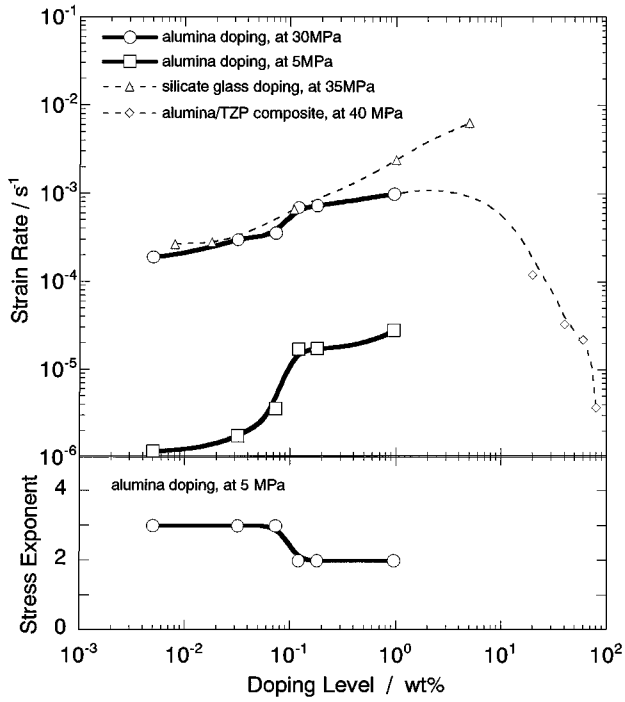

Figure 7 Variation in strain rate (a) and stress exponent (b) with doping levels at 30 MPa for $n = 2$ region and 5 MPa for $n = 3$ region for high-purity TZP. The data for alumina/TZP composite [17] and TZP doped with silicate glass [13] are also plotted. Alumina doping increases the strain rate at both stresses up to 0.1 wt % and shows a tendency toward saturation above that. Around this doping level, the stress exponent at low stresses also changes from three to two. In contrast to alumina doping, silicate glass doping does not show a tendency toward saturation above 0.1 wt % because of glassy pocket formation at the triple points.

the $n = 3$ region for high-purity TZP as shown in Fig. 2. Alumina doping increases the strain rate at both stresses up to 0.1 wt % and shows a tendency toward saturation above that. Around this doping level, the stress exponent at low stresses also changes from three to two, as shown in Fig. 7b. This behavior means that the deformation mechanism at low stresses in high-purity TZP changes into that in low-purity TZP at a 0.1 wt % doping level. Alumina doping of more than 0.1 wt % causes little increase in the strain rate, and if we dope more alumina, the material is considered as an alumina/TZP composite and shows a very low strain rate as indicated by the broken line in Fig. 7a [17].

Fig. 7a also shows the data of Gust *et al.* [13] who studied the doping effect of silicate glass. They used a low-purity powder (total impurity level of more than 0.1 wt %) as a raw material; therefore their material without doping did not show the behavior of high-purity TZP, i.e., only the $n = 2$ region was observed, and they did not discuss the transition from high-purity to low-purity. In contrast to alumina doping, silicate glass doping does not show a tendency toward saturation above 0.1 wt %, because it creates glassy pockets at the triple points (not a grain boundary glassy film as claimed by Ikuhara *et al.* [20]), which enhance the stress relaxation at the triple points.

4.3. Interface reaction control

The present results, i.e., the absence of a grain boundary glassy phase and a stress exponent of two or three, suggest that the deformation is grain boundary sliding with grain switching [21] accommodated by diffusion creep controlled by interface reaction, i.e., vacancy formation and absorption at the grain boundaries [22]. Assuming that the reaction rate is proportional to the stress, the site density of the reaction should be proportional to the second power of the stress at low stresses and proportional to the stress at high stresses in pure TZP. Alumina doping may enhance the transition from

low stresses to high stresses through affecting the interface reaction by alumina ion segregation at the grain boundaries, and that more than 0.1 wt % results in a single region with a stress exponent of two.

The transition takes place at a doping level of 0.1 wt %. If we assume that all aluminum ions locate at the grain boundaries, we can roughly calculate the ratio of the grain boundary area covered by aluminum ions as 20% using the following equation,

$$W = \frac{fd}{2S_v a}. \quad (2)$$

Here aluminum ion is assumed to cover the TZP grain boundary with the width of alumina unit cell a accompanied with two oxygen ions, f is the volume fraction of alumina calculated from the doping level, S_V is the grain boundary area in a unit volume (3.30 [30]) and d is the grain size of the TZP matrix. Considering that the TZP grain boundary has already been covered by yttrium, aluminum can occupy up to 20% of the grain boundary at high temperatures by pushing yttrium aside.

Alumina doping of more than 0.1 wt % is expected to cause precipitation of alumina phase but not to increase the area fraction of the grain boundary occupied by aluminum ion. That is, at the doping level where grain boundaries become saturated with yttrium, the deformation behavior is expected to change from that at low stresses in high-purity TZP to that in low-purity TZP.

Such a change in deformation behavior has been reported in the case of yttria doping in high-purity alumina. Alumina shows quick grain growth during creep and thus shows a continuous decrease in strain rate with time. However, Gruffel and Carry found a constant strain rate-plateau-regime during creep in yttria-doped alumina [31]. They also found that, during the plateau regime, yttrium segregation at the grain boundaries increased with grain growth, and that the end of the plateau regime corresponded to the saturation of segregation and the start of precipitation of yttria garnet [32]. Future work is required to understand the details of the interface reaction at the grain boundaries with dopant segregation close to its saturation level.

4.4. Yttrium segregation

For the observed denuded zone, we calculated the diffusion distance of yttrium using a volume diffusion constant for cubic zirconia, $D_v = 2.7 \times 10^{-5} \exp[-423\ \text{kJ mol}^{-1}/RT]\ \text{m}^2\ \text{s}^{-1}$ measured by Oishi *et al.* [27]. For sintering at 1673 K 2 h and 1773 K 10 h, the diffusion distance is calculated to be 100 and 600 nm, respectively, but the identical and small widths of 30 nm are observed as seen in Fig. 5.

Here we examine the idea that this denuded zone was created during cooling from the sintering temperature because we used a small cooling rate of 10 K/min to avoid cracking. The diffusion distance during cooling from 1673 to 1573 K in 10 min is calculated to be 20 nm, which is close to the observed width. This means that during high temperature creep, we can expect the equilibrium distribution of yttrium, though after slow cooling, we observed denuded zones.

5. Conclusions

High-purity TZP with less than 0.07 wt %Al_2O_3 and a grain size of 0.4 μm had two deformation regions: the low stress region had a stress exponent of three and an apparent activation energy of 640 kJ/mol, and the high stress region had two and 460 kJ/mol. On the other hand, TZP containing more than 0.12 wt %Al_2O_3 with the same grain size had only one region which had a stress exponent of two and an activation energy of 480 kJ/mol. The region of diffusion control with a stress exponent of one was not observed in any samples.

High resolution transmission electron microscopy revealed the absence of an amorphous grain boundary phase with 0.18 wt %Al_2O_3 doping. Very few grain boundary triple points possessed a glassy pocket, which consisted of silicate glass. EDS analyses near the grain boundaries revealed that yttrium was segregating at the grain boundaries with denuded zones of 30 nm width. This denuded zone was created during slow cooling from the sintering temperature.

References

1. F. WAKAI, S. SAKAGUCHI and Y. MATSUNO, *Adv. Ceram. Mater.* **1** (1986) 259.
2. A. H. CHOKSHI, *Mater. Sci. Eng.* **A166** (1993) 119.
3. F. WAKAI and T. NAGANO, *J. Mater. Sci. Lett.* **7** (1988) 607.
4. *Idem., J. Mater. Sci.* **26** (1991) 241.
5. F. WAKAI, S. SAKAGUCHI, N. MURAYAMA, Y. KODAMA and N. KONDO, *Trans. Mater. Res. Soc. Jpn.* **16B** (1994) 947.
6. T. G. NIEH, C. M. MCNALLY and J. WADSWORTH, *Scr. Metall.* **22** (1988) 1297.
7. T. G. NIEH and J. WADSWORTH, *Acta Metall. Mater.* **38** (1990) 1121.
8. M. NAUER and C. CARRY, *Scr. Metall. Mater.* **24** (1990) 1459.
9. A. LAKKI, R. SCHALLER, M. NAUER and C. CARRY, *Acta Metall. Mater.* **41** (1993) 2845.
10. D. M. OWEN and A. H. CHOKSHI, in "Science and Technology of Zirconia V" (Technomic Pub., 1993).
11. C. J. HWANG and I-W. CHEN, *J. Amer. Ceram. Soc.* **73** (1990) 1626.
12. Y. YOSHIZAWA and T. SAKUMA, *ibid.* **73** (1990) 3069.
13. M. GUST, G. GOO, J. WOLFENSTINE and M. L. MECARTNEY, *ibid.* **76** (1993) 1681.
14. K. KAJIHARA, Y. YOSHIZAWA and T. SAKUMA, *Acta Metall. Mater.* **43** (1995) 1235.
15. F. WAKAI and H. KATO, *Adv. Ceram. Mater.* **3** (1988) 71.
16. T. G. NIEH, C. M. MCNALLY and J. WADSWORTH, *Scr. Metall.* **23** (1989) 457.
17. I. W. CHEN and L. A. XUE, *J. Amer. Ceram. Soc.* **73** (1990) 2585.
18. T. STOTO, M. NAUER and C. CARRY, *ibid.* **74** (1991) 2615.
19. S. PRIMDAHL, A. THOLEN and T. G. LANGDON, *Acta Metall. Mater.* **43** (1995) 1211.
20. Y. IKUHARA, P. THAVORNITI and T. SAKUMA, *Acta Metall.* **45** (1997) 5275.
21. M. F. ASHBY and VERRAL, *ibid.* **21** (1973) 149.
22. E. ARZT, M. F. ASHBY and R. A. VERRAL, *ibid.* **31** (1983) 1977.
23. R. RAJ and C. K. CHYUNG, *ibid.* **29** (1981) 159.
24. F. WAKAI, *Acta Metall. Mater.* **42** (1994) 1163.
25. W. K. BURTON, N. CABRERA and F. C. FRANK, *Phil. Trans. R. Soc.* **A243** (1951) 299.
26. W. R. CANNON and T. G. LANGDON, *J. Mater. Sci.* **23** (1988) 1.

27. Y. OISHI, K. ANDO and Y. SAKKA, *Adv. Ceram.* **7** (1983) 208.
28. M. KUSUNOKI and Y. IKUHARA, *Ceramics* **30** (1995) 404.
29. A. DIMÍNGUEZ-RODRÍGUEZ, A. BRAVO-LEÓN, J. D. YE and M. JIMÉNEZ-MELENDO, *Mater. Sci. Eng.* **A247** (1998) 97.
30. E. E. UNDERWOOD, in "Quantitative Microscopy" (McGraw-Hill, 1968) p. 5.
31. P. GRUFFEL and C. CARRY, Proc. 11th Int. Symp. Metallurgy and Materials Science (Riso National Lab., 1990) p. 305.
32. P. GRUFFEL and C. CARRY, *J. Euro. Ceram. Soc.* **11** (1993) 189.

Received 30 July 1998
and accepted 24 February 1999